MRS Advances (2024) 9:2–6
https://doi.org/10.1557/s43580-023-00619-w

ORIGINAL PAPER

Effect of Sb and Ag additions on the melting and solidification of Sn-Bi solder alloys

Yifan Wu[1] · Hannah N. Fowler[1] · Nathaniel Weddington[1] · John E. Blendell[1] · Carol A. Handwerker[1]

Received: 30 May 2023 / Accepted: 13 July 2023 / Published online: 27 July 2023

Abstract

Low temperature solders based on tin-bismuth (Sn-Bi) are used as substitutes for tin-silver-copper (Sn-Ag-Cu, SAC) alloys, reducing warpage-induced defects and reflow temperature. Understanding the effects of microalloying elements on the solder mechanical, microstructural, and thermodynamic properties constitute an essential part of alloy design. This study focuses on the changes in melting and solidification behavior of near-eutectic Sn-Bi alloys with antimony (Sb, 0.5–2 wt%) and silver (Ag, 0–1 wt%) additions. Our differential scanning calorimetry studies show that addition of Sb increases the melting temperature of the alloy and reduces the amount of undercooling, while the addition of Ag has a minimal effect on the melting and solidification behavior. Of note is the melting temperature between the initial melting of as-solidified solders and subsequent cycles in Sb-containing alloys decreases. Microstructural and thermodynamic analysis reveals that the distribution of solute Sb atoms in as-received, more rapidly solidified alloys compared with reflowed alloys is likely the cause of the difference in melting behavior.

Abbreviations

SAC	Sn-Ag-Cu alloys
IMC	Intermetallic compound
DSC	Differential scanning calorimetry
EDS	Energy dispersive X-ray analysis
EPMA	Electron probe microanalysis
WDS	Wavelength dispersive spectroscopy
ICP-MS	Inductively coupled plasma mass spectroscopy

Elements

Ag	Silver
Au	Gold
Bi	Bismuth
Co	Cobalt
Cu	Copper
In	Indium
Ni	Nickel
Pb	Lead
Zn	Zinc

Introduction

While Sn-Pb solder alloys had been widely used in the microelectronics industry for their low melting temperatures(183 °C), low cost, good wettability, and high reliability, concerns over lead's impact on human health and the environment have led to the banning of the use of lead in electronic packaging with the issuing of regulations such as RoHS and WEEE. The lead-free alternative, Sn-Ag-Cu (SAC), which has since become the industry standard, has the major disadvantage of having a high melting temperature (217 °C). As integrated circuits grow thinner and more heterogeneous, the high reflow temperature of SAC alloys can cause serious component warpage and manufacturing-induced damage to the solder joints [1]. Well-known examples of warpage-induced defects include head-on-pillow, head-on-pillow open, and bridging defects, which can cause either open circuit or short circuit failures [1].

Eutectic Sn-Bi alloy rose to prominence in the research of low temperature soldering solutions due to its low eutectic temperature (138 °C), low cost, and reliable mechanical performance at low strain rates. However, being highly strain rate dependent, Sn-Bi alloys perform poorly at high strain rates, e.g., in drop-shock testing. Previous studies on SAC alloys have shown that small amounts of microalloying elements addition can lead to marked improvements in aging resistance and reliability [2, 3]. Concerns over Sn-Bi alloys' poor mechanical reliability in drop-shock naturally led to

✉ Yifan Wu
wu1394@purdue.edu

[1] Purdue University, West Lafayette, USA

many studies attempting to improve the mechanical performance via microalloying, particularly in understanding the relationship between microalloying elements and their effects on the microstructural evolution and intermetallic compound (IMC) growth Sn-Bi solder [4–10]. It is recognized that the addition of Ag introduces Ag_3Sn IMCs in the solder and refines the microstructure [8]. The presence of Ag in the solder also reduces the rate of Cu_6Sn_5 growth at the solder-Cu interface. Addition of Cu has also been shown to refine the solder microstructure, with Cu_6Sn_5 forming in the matrix. Additions of Zn, Ni, In, Sb, Co, and Au have also been studied for their effect on IMC growth at the solder-Cu surface finish interface, as described in the extensive review by Wang et al. of microalloying effects in Sn-Bi solders [11].

Of the many microalloying elements mentioned above, Sb has attracted particular attention for its unique ability to greatly increase the ductility of the Sn-Bi alloy while retaining its tensile strength [4, 6, 7, 10]. Microstructural and elemental analysis reveals that a combination of Sb in solid solution in Sn and precipitation of SnSb IMC at Sn-Bi boundaries is likely contributing to the improved mechanical properties [5]. An additional factor is the interaction between alloy composition, solidification behavior and microstructure. As in SAC alloys, the degree of undercooling provides information on the nucleation behavior from molten solders and the origin of specific microstructures, an integral part in the refinement of the mechanical properties and overall design of the reflow process [12]. In this study, we examine near-eutectic Sn-Bi alloys with Sb and Ag addition to study the relationship between microalloying, the melting and solidification behavior of the solder alloys and how they are linked to the microstructure of the alloy.

Experimental

A series of six Bi-42Sn-*x*Sb-*y*Ag ($x=0.5$, 1, 2 and $y=0$, 1) solder alloys in the form of 500 µm spheres were obtained from the Scientific Alloys corporation. The spheres were fabricated by dropping the alloy melt into a liquid, and so the cooling rate is much faster than the rates typically seen in during reflow or differential scanning calorimetry (DSC) testing. Prior to DSC testing, the elemental composition of the samples was verified using inductively coupled plasma mass spectroscopy (ICP-MS). The exact elemental composition of each alloy obtained from ICP-MS is within an acceptable range of the requested Bi-42Sn-*x*Sb-*y*Ag ($x=0.5$, 1, 2 and $y=0$ or 1) with ± 2 wt% Sn, ± 0.1 wt% Sb, and ± 0.3 wt% Ag [5]. Overall, all alloys (except for the Bi-42Sn-2Sb-1Ag alloy) contain more Sn and less Bi than their nominal compositions. In terms of microalloying elements, the concentrations of Sb are close to what is expected, while the concentration of Ag showed greater variability. See Supplementary 1 for the table of measurements.

The melting and solidification behavior of the alloys were measured using a TA Q2000 DSC in Tzero hermetic aluminum pans. A single solder sphere was used in each DSC run. Each DSC cycle started at 60 °C and was heated to 200 °C with a ramp rate of 20 °C/min. The sample pan was then isothermally held at 200 °C for 5 min to ensure complete melting/dissolution of IMCs before being cooled down to 60 °C at a ramp rate of 20 °C/min. Three samples were tested for each alloy with three DSC cycles per experiment.

Samples form the DSC experiments were mounted in epoxy for microstructural analysis. Two other sets of metallographic samples were prepared for: (i) as-received solder alloys and (ii) solder alloys after one DSC cycle for each alloy to compare the microstructures after one and three thermal cycles. Metallographic samples were mechanically polished to a final polish of 0.05 µm diamond suspension and were imaged using a FEI Quanta 650 FEG scanning electron microscope. Energy Dispersive X-ray Analysis (EDS) and electron probe microanalysis (EPMA) wavelength dispersive spectroscopy (WDS) were used to identify the compositions of the IMC phases and their relationships to β-Sn and Bi phase.

Results and discussion

Table 1 shows the DSC results for Cycle 1 and Cycle 2 of the six alloys tested. Cycles 3 was identical to Cycle 2 for all alloys and are not listed here. The solidus is the temperature at which the first liquid forms on heating. The liquidus is

Table 1 Liquidus and solidus temperatures of Bi-42Sn-*x*Sb-*y*Ag ($x=0$, 0.5, 1, 2 and $y=0$ or 1) alloys

	0Sb-0Ag	0.5Sb	1Sb	2Sb	0Sb-1Ag	0.5Sb-1Ag	1Sb-1Ag	2Sb-1Ag
Solidus temperature: cycle 1 (°C)	136.3	139.9	140.8	142.8	138.2	139.3	139.9	141.5
Liquidus temperature: cycle 1 (°C)	121.0	125.0	130.5	138.6	123.9	126.9	131.1	137.6
Degree of undercooling: cycle 1 (°C)	15.3	14.9	10.3	4.2	14.3	13.6	8.8	3.9
Solidus temperature: cycle 2 (°C)	136.1	138.5	138.8	138.7	138.0	137.7	137.8	137.9
Liquidus temperature: cycle 2 (°C)	121.0	127.2	132.9	138.7	124.1	127.8	130.1	137.9
Degree of undercooling: cycle 2 (°C)	15.1	11.3	5.9	0	13.9	9.9	7.7	− 0.1

the temperature of the first solid forms on cooling. Based on the observed liquidus and solidus temperatures, a few observations can be made. First, with increasing amount of Sb addition, the melting temperature of the alloy increases from the eutectic 136.3 °C to 142.8 °C (with 2 wt% Sb addition) as expected from the phase diagram. The addition of Ag into the eutectic Sn-Bi alloy slightly increases the melting temperature to 138.2 °C, while the addition of Ag into Sn-Bi-Sb ternary alloys slightly lowers the melting temperature. The solidification temperature also increases with increasing amount of Sb but at a higher rate than the melting temperatures, resulting in a decrease in the degree of undercooling from 15 °C (Sn-58Bi) to 4 °C (2 wt% Sb addition) (Fig. 1).

Of particular interest is that there is a significant difference in the melting behavior between the initial thermal cycle for the as-received Sb-containing alloys and subsequent cycles across all alloy compositions. Namely, there is a decrease in the onset temperature for melting and a change in the shape of the melting peak. This decrease in the melting temperature, together with the increase in the solidification temperature with increasing amount of Sb addition, produces a striking *negative* amount of undercooling in the alloys with 2 wt% Sb as seen in Sup 2. The change in the onset temperature of the melting peak suggests a change in partitioning of the Sb between initial manufacturing and after reflow.

To reveal the underlying mechanism for the change in the melting behavior, microstructures of each sample were analyzed at three intervals in the DSC study: as received, after the first thermal cycle, and after the third thermal cycle. Figure 2a and g show the microstructure of the Sn-Bi alloy with 0.5 wt% Sb addition. The as-received sample has a much coarser microstructure compared to the ones after thermal cycling. In addition, no dendrites can be seen in the as-received sample and the microstructure is more homogeneous. After thermal cycling, fine dendrites can be seen throughout the sample, while no SnSb intermetallic phases were observed since this composition is within the room temperature solubility limit of Sb in β-Sn. Samples with Ag additions show similar as-received microstructure, with the distinction that fine Ag_3Sn IMC particles are seen throughout the microstructure in Ag-containing alloys, as shown in Fig. 2b and c.

Samples with 1 wt% Sb addition show no significant microstructural differences in the β-Sn and Bi phases from samples with 0.5 wt% Sb addition with the exception that fine SnSb IMC particles are observed in the β-Sn phase at β-Sn-Bi phase boundaries throughout the 1 wt% Sb microstructure in the as-received state and after thermal cycling. However, a significant change in the microstructure starts to emerge in samples with 2 wt% Sb addition. As shown in Fig. 2c for the Bi-42Sn-2Sb-1Ag alloy, the microstructure of the as-received alloy is similar to Bi-42Sn-1Sb as-received sample. However, the microstructure of the 2 wt% Sb alloy after the thermal cycling (Fig. 2i) shows marked differences. Large SnSb IMC particles have formed near the edge of the sample after thermal cycling as seen in Supplementary 3. Given the size and morphology of the SnSb particles, it is

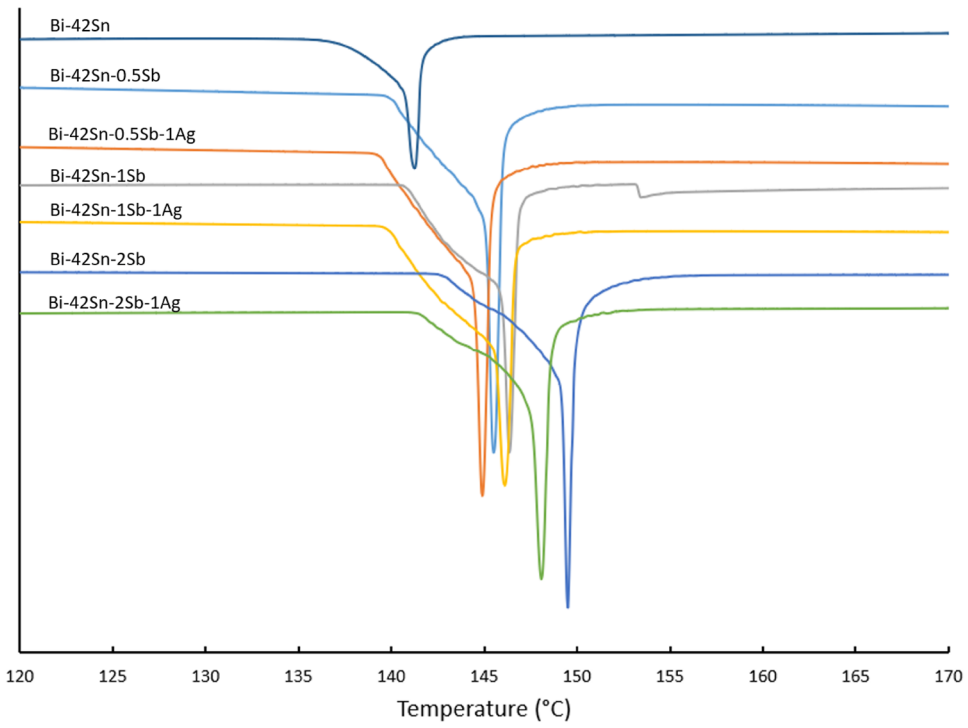

Fig. 1 DSC melting peaks for the as-received Bi-42Sn-*x*Sb-*y*Ag alloys

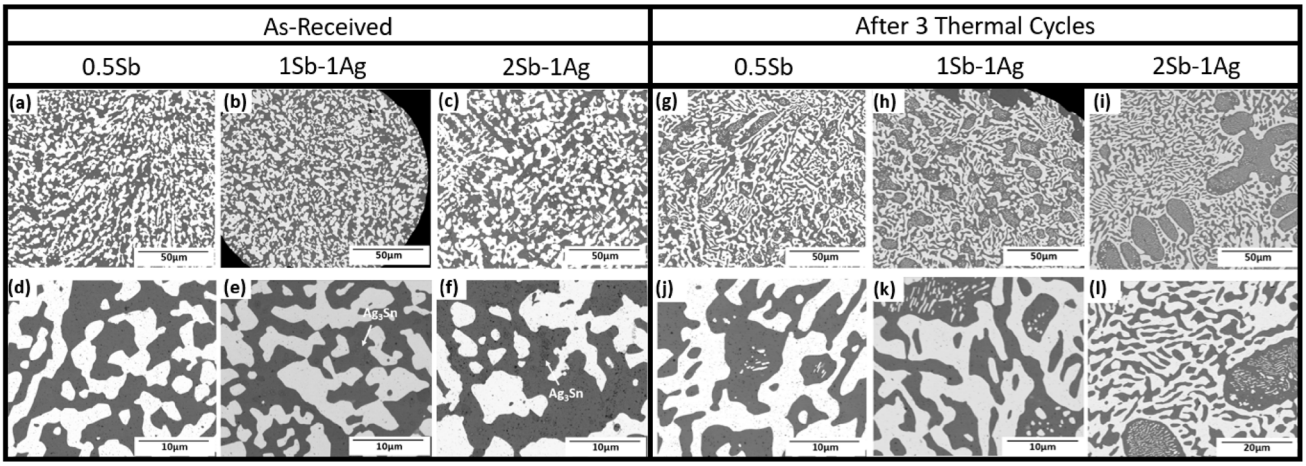

Fig. 2 Microstructures of Bi-42Sn-*x*Sb solder alloy ($x = 0.5, 1.0, 2.0$): **a**–**f** as-received liquid-cooled spheres and **g**–**l** after three thermal cycles at a ramp rate of 20 °C/min with microstructures similar to those seen after reflow

expected that they formed either as the first phase to solidify from the melt during cooling or as undissolved particles in the liquid during the isothermal hold at 200 °C. Large β-Sn dendrites are observed to form with the large SnSb particles acting as nucleation sites and leading to a 4 °C undercooling. At lower Sb compositions, it appears that SnSb particles do not form in the melt and therefore, are not present to act as nucleation agents from the melt. From these experiments it is not clear what serve as nucleating agents for dendrites at lower Sb compositions that activate at larger undercooling [13].

As noted previously, there are no SnSb IMC particles in Bi-42Sn-0.5Sb samples, with EPMA-WDS maps showing Sb in solid solution within β-Sn phase in Fig. 3. In contrast, samples with 1 and 2 wt% Sb additions contain SnSb particles in both the as-received and the cycled samples. In the as-received samples, the SnSb IMC particles are distributed in a more homogeneous manner throughout the sample. The SnSb particles in the cycled samples are predominantly seen within the Sn dendrites rather than at Sn-Bi phase boundaries within the eutectic, and the particles are fine, similar to what is seen previously in samples after reflow [5]. In the cycled 2 wt% Sb samples, there are both large (> 20 μm) SnSb particles, and the fine SnSb particles within the Sn dendrites. The large (> 20 μm) SnSb particles are not observed in the as received samples, likely due to the substantially higher cooling rate during the fabrication of the solder spheres.

One distinctive difference between the as-received and thermal-cycled microstructures in every alloy is the clear lack of dendrites in the as-received samples. This lack of Sn dendrites can be attributed to the manufacturing condition of the solder balls. To our knowledge, in the fabrication of the solder balls, the alloys are heated to a high temperature to ensure complete homogenization before being quenched in an unspecified liquid as 500 μm solder balls. The rapid cooling rate appears to result in a supersaturation of Sb in β-Sn phase, which raises the initial melting temperatures. In the

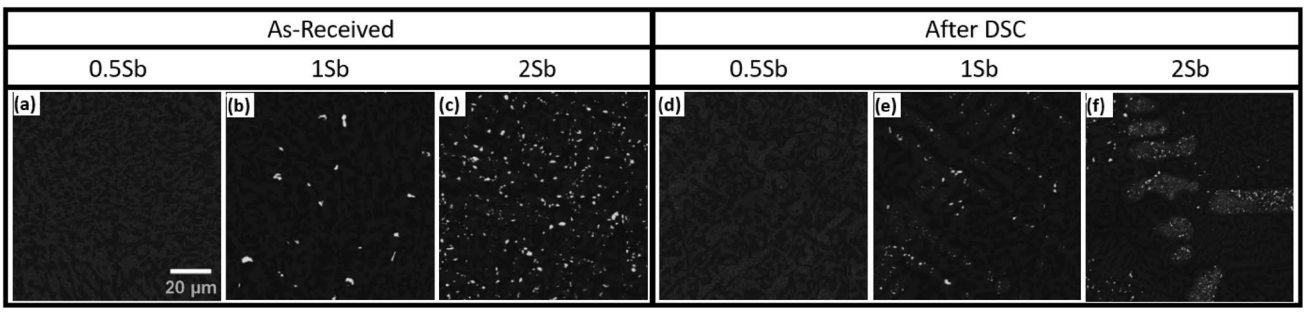

Fig. 3 EPMA-WDS maps of the Sb distribution in liquid-cooled as-received samples and samples after DSC at a ramp rate of 20 °C/min. The 0.5Sb images **a** and **d** show Sb in solution with Sn as a light grey phase. The 1Sb and 2Sb samples **b**, **c**, **e**, and **f** show bright white SnSb IMC particles

DSC cycling, samples are cooled more slowly (20 °C/min). As a result, after the first thermal cycle in DSC, such differences are eliminated and all subsequent cycles demonstrate identical melting behavior.

Conclusion

In this study the effect of Sb and Ag addition on the melting and solidification behavior of near-eutectic Sn-Bi alloys and their microstructures was determined. It was found that the addition of Sb increases both the melting and the solidification temperature of the alloy while reducing the amount of undercooling. The addition of Ag, comparatively, has a less significant effect. A change in the melting temperature between as-received samples and thermal-cycled samples was recorded for alloys of all compositions. Nucleation of Sn on large SnSb shows low undercooling overall compared with SAC.

Supplementary Information The online version contains supplementary material available at https://doi.org/10.1557/s43580-023-00619-w.

Data availability All data generated or analyzed during this study are included in this published article [and its supplementary information files].

Declarations

Conflict of interest On behalf of all authors, the corresponding author states that there is no conflict of interest.

References

1. S. Mokler, R. Aspandiar, K. Byrd, O. Chen, S. Walwadkar, *The Application of Bi-Based Solders for Low Temperature Reflow to Reduce Cost While Improving SMT Yields in Client Computing Systems* (Intel Corporation, Hillsboro, 2016)
2. M.D. Hasnine et al., Nanomechanical Characterization of SAC Solder Joints-Reduction of Aging Effects Using Microalloy Additions, in *2015 IEEE 65th Electronic Components and Technology Conference (ECTC)*. (IEEE, Manhattan, 2015)
3. Y. Zhang et al., The Effects of SAC Alloy Composition on Aging Resistance and Reliability, in *2009 59th Electronic Components and Technology Conference*. (IEEE, Manhattan, 2009)
4. S. Sakuyama, T. Akamatsu, K. Uenishi, T. Sato, Effects of a third element on microstructure and mechanical properties of eutectic Sn-Bi solder. Trans. Jpn. Inst. Electron. Packag. **2**, 98–103 (2009). https://doi.org/10.5104/jiepeng.2.98
5. H.N. Fowler, S.X. Tay, J. Blendell, C.A. Handwerker, Microalloying effects of Sb and Ag on the microstructural evolution of eutectic Sn-Bi alloys. MRS Adv. **2023**, 1–5 (2023). https://doi.org/10.1557/S43580-022-00472-3
6. F. Yang, L. Zhang, Z.Q. Liu, S.J. Zhong, J. Ma, L. Bao, Properties and microstructures of Sn-Bi-X lead-free solders. Mater. Today Proc. (2016). https://doi.org/10.1155/2016/9265195
7. J.G. Li, X. Ma, M.B. Zhou, X. Ning, X.P. Zhang, Effects of Sb Addition on the Microstructure and Mechanical Performance of Sn58Bi Based Alloys and the Solder Joints, in *Proceedings 2018 19th International Conference on Electronic Packaging Technology, ICEPT 2018*. (IEEE, Manhattan, 2018), pp.457–461
8. M. Mccormack, H.S. Chen, G.W. Kammlott, S. Jin, Significantly improved mechanical properties of Bi-Sn solder alloys by Ag-doping. J Electron Mater **26**, 954–958 (1997). https://doi.org/10.1007/S11664-997-0281-7
9. O. Mokhtari, H. Nishikawa, Correlation between microstructure and mechanical properties of Sn-Bi-X solders. Mater. Sci. Eng., A **651**, 831–839 (2016). https://doi.org/10.1016/j.msea.2015.11.038
10. C. Zhang, J. Zhou, S.D. Liu, G.T. Qian, F. Xue, Effect of Sb content on properties of Sn−Bi solders. Trans Nonferrous Met Soc China **24**, 191 (2014). https://doi.org/10.1016/S1003-6326(14)63046-6
11. F. Wang, H. Chen, Y. Huang, L. Liu, Z. Zhang, Recent progress on the development of Sn-Bi based low-temperature Pb-free solders. J. Mater. Sci. Mater. Electron. **30**, 3222–3243 (2019)
12. A.F. da Silveira, W.B. de Castro, B.A. Luciano, C.S. Kiminami, Microstructure of under-cooled Sn-Bi and Al-Si alloys. Mater. Sci. Eng., A **375–377**, 473–478 (2004). https://doi.org/10.1016/J.MSEA.2003.10.017
13. K.N. Subramanian, D. Swenson, The Effects of Suppressed Beta Tin Nucleation on the Microstructural Evolution of Lead-Free Solder Joints, in *Lead-Free Electronic Solders*. (Springer, Cham, 2007), pp.39–54